SolarPACES 2023, 29th International Conference on Concentrating Solar Power, Thermal, and Chemical Energy Systems

Operations, Maintenance, and Component Reliability

https://doi.org/10.52825/solarpaces.v2i.913

Published: 24 Jul. 2024

Advanced Controllers for Heat Transfer Fluid Mass Flow Rate Control in Solar Tower Receivers

Cody B. Anderson[1,2], Giancarlo Gentile[2,*], Alessandro Longhi[3], Francesco Casella[3], Michael E. Cholette[1], and Giampaolo Manzolini[2]

[1] Queensland University of Technology, Mechanical, Medical and Process Engineering School

[2] Politecnico di Milano, Dipartimento di Energia

[3] Politecnico di Milano, Dipartimento di Elettronica

* Correspondence: Giancarlo Gentile, giancarlo1.gentile@polimi.it

Abstract. Efficient control strategies for managing the mass flow rate (MFR) of heat transfer fluids (HTF) during cloud transients in Solar Tower receivers play a pivotal role in optimizing plant profitability and receiver durability. This study focuses on the performance and durability of Solar Tower receivers during cloud transients. It evaluates adaptive feedback and feedforward control methods, which adjust the flow rate of heat transfer fluids based on real-time measurements of direct normal irradiance (DNI), receiver outlet and receiver panel outlet temperatures. The effectiveness of an aggressive all-sky and conservative clear-sky control strategy is explored against a conventional PI controller, emphasizing energy efficiency and receiver longevity. Simulations using a thermal Modelica model resembling a 100 MW_{el} Crescent Dunes-like solar tower plant reveal that both advanced controllers provide precise setpoint tracking, while the PI controller struggles. The conservative controller which has a cloud standby mode prevents overheating during cloud transients by using a clear sky mass flow rate, while the aggressive controller uses the receiver panel outlet temperatures to correct for upstream tube temperature variations allowing for fast tracking correction and disturbance rejection, albeit with slight overshoots. Furthermore, the controllers significantly decrease the creep-fatigue damage accumulated in the receiver panels during cloudy days, due to limiting the increase in wall temperature spikes when cloud events end. Overall, this study underscores the pivotal role of HTF mass flow rate control systems in influencing receiver system failure modes and longevity and offers a new tool in controller design and operation assessment.

Keywords: Control Systems, Concentrated Solar Thermal, Modelica, Lifetime Prediction

1. Introduction

Efficient control strategies for managing the mass flow rate (MFR) of heat transfer fluids (HTF) in solar tower receivers during cloud transients are essential for optimizing plant profitability and extending the operational life of receiver components. Disturbances such as the passage of clouds and variations in dynamic characteristics, including response rate and dead time, can introduce challenges in maintaining desired outlet temperatures, posing a risk of receiver tube degradation. These control systems are designed to achieve a setpoint for the receiver HTF outlet temperature by regulating the HTF flow rate. Elevated outlet temperatures in receivers can accelerate the deterioration of receiver components, while lower temperatures can reduce the entropy within thermal energy storage tanks, thereby affecting plant performance.

Historically, conservative control strategies have been adopted, where HTF flow rates are adjusted to mimic clear-sky conditions during cloud transients [1]. This approach mitigates temperature spikes in the receiver when cloud events dissipate but may result in a significant revenue loss due to prolonged periods of HTF delivery at temperatures lower than the nominal setpoint. Notably, Nouri B. et al. [2] harnessed spatially resolved direct normal irradiance (DNI) data from all-sky imagers to offer cloud transient nowcasting, optimizing revenue generation under all sky conditions. In the analysis of tracking errors and disturbance rejection, Kannaiyan S. and Bokde N. [3] identified limitations in a PI feedback controller combined with a static feedforward compensator for parabolic trough collectors. Gentile et al. [4] highlighted that PI feedback controllers led to significant HTF temperature spikes during cloud transients, resulting in substantial creep damage accumulation in the receiver. Thus, the performance of an HTF controller can significantly impact the receiver's outlet temperature, revenue, and ultimately, the lifetime of receiver components. However, existing studies often overlook the comprehensive effect of tube temperature profiles on receiver component longevity, and the few that do consider this aspect often employ rudimentary feedback controllers that are not state-of-the-art.

This study investigates two advanced control structures: an aggressive controller designed to operate in all-sky conditions and a robust controller tailored exclusively for clear-sky conditions. Both controllers regulate the MFR based on the measured HTF outlet temperature (feedback signal) and real-time measurements of the direct normal irradiance (DNI) incident on the solar field (feedforward signal). The case study evaluates each controller's performance using a 100 MW_{el} concentrated solar thermal (CST) tower plant resembling the Crescent Dunes facility over a cloud riddled DNI profile generated using Copylot. The advanced controllers are compared against the PI controller described in [4] (hereafter referred to as the base controller), considering energy performance and receiver lifetime as key performance indicators. This innovative approach integrates receiver lifetime and thermal models to comprehensively assess the impact of controller designs. The overarching objective of this project is to quantify the influence of receiver controller strategies on receiver operation and maintenance practices, offering valuable insights for the CSP community.

2. Methodology

The methodology, as illustrated in Figure 1, provides a structured framework for evaluating the influence of HTF controllers on the operational lifetime of solar receivers. To quantify the cumulative damage resulting from creep and fatigue, the lifetime assessment approach from [4] is employed. This assessment method considers creep-fatigue damage, considering material plasticity and stress relaxation due to creep, which are calculated based on the thermo-elastic stress history simulated using the dynamic 2D thermal receiver model, SolarReceiver2D [5].

The Modelica receiver model is a versatile tool that accommodates various receiver geometries, materials, HTFs, and control configurations. This model is instrumental in simulating the thermal efficiency of the receiver and the temperature profiles experienced by the receiver tubes and HTF, tailored to specific flux maps and solar-field designs. Within SolarReceiver2D, HTF controllers are designed and tuned allowing for a detailed analysis of their impact on receiver performance.

Simulation of the receiver's behaviour is facilitated through the utilization of a CST design generated with SolarPILOT [6], complemented by its Python application programmable interface, CoPylot [7]. This integrated approach enables the generation of receiver flux maps and the emulation of "measured" DNI data, which are essential inputs for feedforward control strategies, particularly in scenarios involving cloud cover over the course of a day.

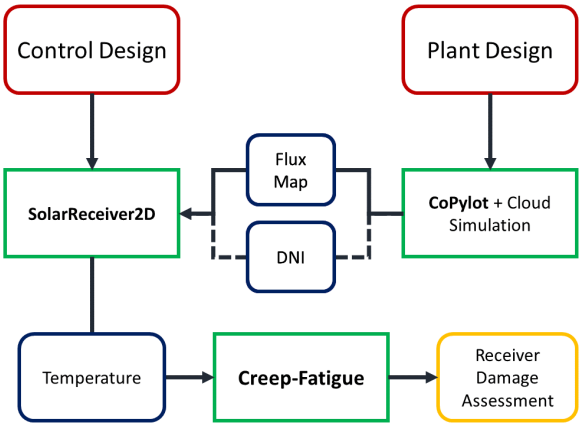

***Figure 1**. HTF MFR Controller-Receiver Damage Assessment Methodology*

3. Case Study – Aggressive and Conservative Controllers

Two advanced and a base feedback only controller were tested against a solar tower (ST) plant like Crescent Dunes one (100 MW_{el}). Controllers were tasked with adjusting the receiver's HTF MFR (Solar Salt) to reach a set receiver outlet temperature (T_{ref}) using either receiver outlet HTF temperature, receiver panel(s) outlet temperature, and simulated DNI measurements from the field. The two advanced controllers (shown in Figure 2) can be described as an *aggressive* all-sky controller similar to that of that attempts to correct cloud disturbances similar to that designed by C. Maffezzoni et al. [8], and a conservative clear-sky only controller similar to that used by R. Bradshaw et al. [1] that attempts to reach setpoint during clear sky or low disturbance periods. During large cloud passovers a clear sky mass flow rate is used to prevent overheating of the receiver panels. Performance of each controller is compared to a base feedback controller that was used in a previous creep-fatigue assessment study [4]. Where receiver tube temperature distributions are assessed for each controller across a cloudy day using SolarReceiver2D.

Both advanced controller systems made use of a feedforward estimate MFR controller from an average *measured* DNI as opposed to the *actual* incident irradiance on the receiver. Where the average measured DNI (DNI_{avg}) is the actual DNI disturbance from 8 points within the field with random (±5%) noise subtracted. The uncertainty of DNI attempts to mimic the non-idealised measurements provided to receiver control systems. These DNI measurements are used in conjunction with a feedfoward disturbance compensator that provides an approximate mass flow rate (w_{ff}) based upon Eq 1.

$$w_{ff} = \frac{\mathrm{DNI}_{\mathrm{avg}} A_{sf} \cdot \eta_{rec} \eta_{opt}}{c_{p,\mathrm{avg}} \cdot (\Delta T)} \quad (1)$$

Where A_{sf} is the solar field reflective area, η_{rec} is the receiver thermal efficiency, η_{opt} is the optical efficiency, $c_{p,avg}$ is the average fluid specific heat and ΔT is the temperature difference between the receiver inlet and setpoint temperature. While the feedfoward has been setup to not provide perfect control the compensator will drive the mass flow rate "near" the final equilibrium point where one of two feedback systems will correct the remaining errors.

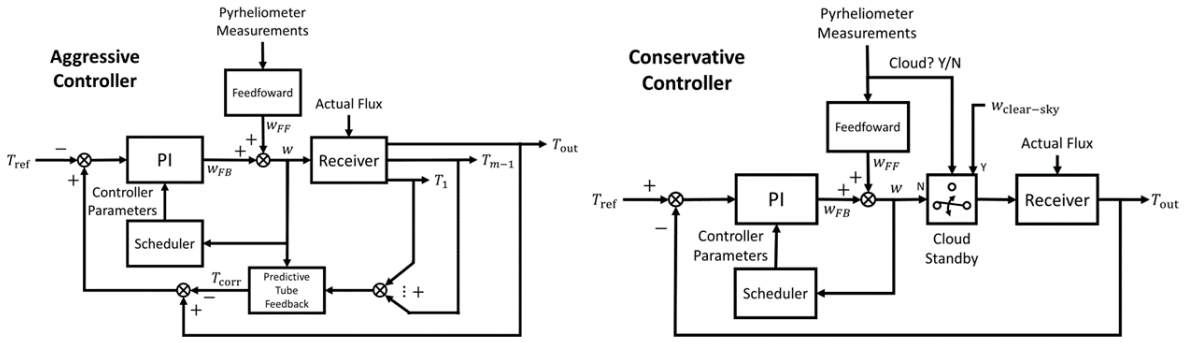

Figure 2. *Controller diagrams. Left. aggressive all-sky. Right. conservative clear sky.*

The conservative controller uses an adaptive feedback PI system that has been tuned using a first order plus delay internal model controller based upon a open loop receiver configuration with a step input at several mass flow rates with corresponding flux maps near the set point temperature. An adaptive feedback system is necessary to react to the variable response rate and dead times that change with the mass flow rate. The adaptive feedback PI system provides adequate tracking when given errors near the ideal mass flow rate. In addition, the controller uses a cloud standby mode which is activate when either a DNI measurement falls below 25% of the clear sky DNI or the outlet temperature falls below 50 K below the set point temperature. When in cloud standby mode the mass flow rate contribution from the feedback and feedfoward systems are ignored and a clear sky mass flow rate is utilised preventing the receiver from overheating after cloud passage over the solar field.

The aggressive controller utilises a cascade feedback controller, containing an adaptive feedback that allows steady-state tracking and error correction, and a tube temperature compensator that provides a feedback correction, T_{cor} to the outlet temperature error. Since any feedback control system using only the outlet temperature cannot provide satisfactory performance when the HTF-temperature function is nonminimum phase. Where these phase effects are due to panel temperatures variations upstream of the outlet that propagate toward the receiver outlet at an approximate speed corresponding to the mass flow rate, thus affecting the receiver outlet temperature with considerable delay [8]. To mitigate the nonminimum phase effect the mass flow rate is recorded and temperature sensors are added at the end of each panel ($T_{1,\ldots,}T_{m-1}$), the outlet temperatures are summed and passed through a compensator that is scaled with the mass flow rate to correct upstream tube temperature effects. The adaptive feedback structure allows for good control of fast and large transients caused by clouds allowing for an all-sky control operation.

3.1 CoPylot Cloud Flux Maps and DNI Measurements

In the absence of real data the solar tower simulation software CoPylot was used to generate and simulate an operating solar tower plant with cloud transients. The 16 clouds were introduced to the solar field from 10:00 AM and varied in velocity, size, opacity, starting position, and direction. The one-day simulation was setup to record direct normal irradiance from 8 positions within the solar field and flux maps for the receiver for 5-minute intervals, as shown in Figure 3. To reduce reliance on a perfect DNI feed forward model random noise was added to the DNI measurements where errors as high as 5 % could occur. Both the flux map and DNI timeseries were used as input for the SolarReceiver2D model.

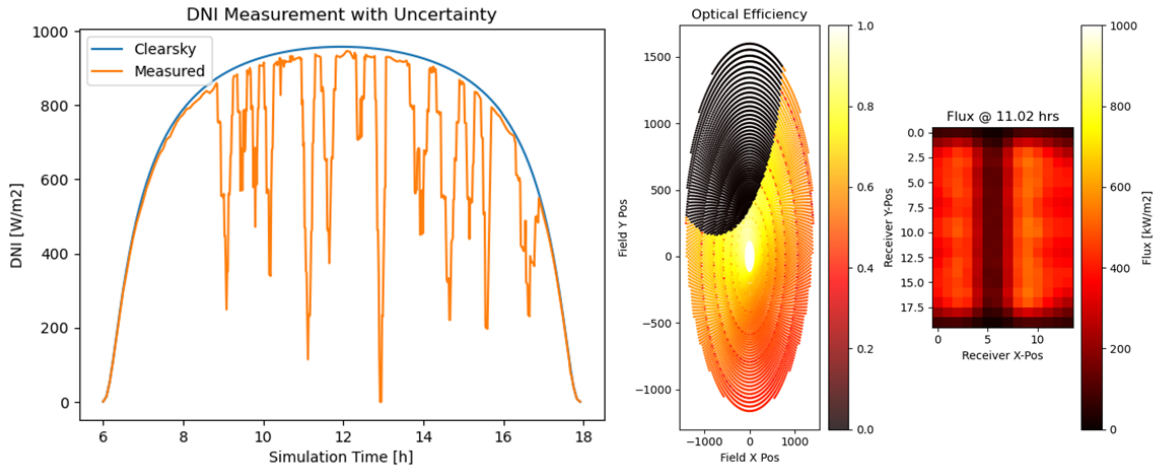

Figure 3. *CoPylot 1 Day Simulation. Left. clearsky and mean pyrheliometer DNI. Middle. solar field optical efficiency with large cloud snapshot. Right. corresponding flux map snapshot*

3.2 SolarReceiver2D Thermo-Mechanical Simulations

Receiver thermal-mechanical properties are retrieved for the one-day DNI/flux map cloud simulations and the three HTF controllers using the thermal receiver Modelica model SolarReceiver2D. Receiver outlet temperature timeseries of the three controllers are plotted in Figure 4 against the set point temperature. Upon inspection the base controller (feedback only) is inadequate at set point tracking and disturbance rejection, causing large oscillations and slow reactions to temperature errors. Whereas the conservative controller shows adequate set point tracking during non-cloudy periods and large oscillations in temperatures below the setpoint during cloud transients. Lastly, the aggressive controller shows excellent set point tracking during clear skies and mild overshoots during cloudy periods.

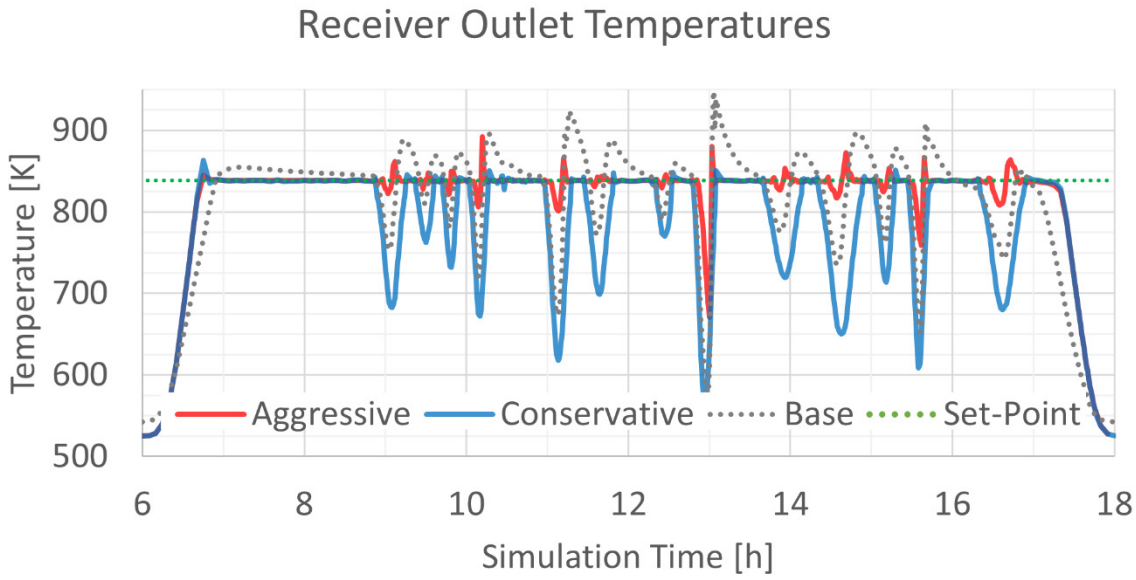

Figure 4. *Outlet Temperature for the Three Controllers*

Performance statistics for the three controllers are reported in Table 1 for the integrated time weighted absolute error (ITAE) to denote tracking error over the simulation, maximum overshoot above the setpoint temperature, and total exergy of the receiver. Analysis shows the aggressive controller has the best tracking response, as denoted by the lowest ITAE followed by the base controller since it also tries to correct for cloud disturbances whereas the

conservative employs a clear sky mass flow rate (higher mass flow rate so lower temperature outlet) causing larger tracking errors. We observe consistent patterns in exergy efficiency when the maximum outlet temperature is limited to the set point temperature. The aggressive controller exhibits the highest exergy efficiency, while the conservative controller records the lowest. Notably, the baseline controller surpasses the conservative one in efficiency. However, it's important to note that any extra work generated beyond what the conservative controller achieves is short-lived, as sustained operation at such elevated temperatures is likely to result in significant degradation. Overshoots for all systems perform as expected with the base controller having the highest due to the inability to react to cloud disturbances in time, and the lowest overshoot being the conservative due to its policy of inaction against cloud transients.

Table 1 Controller Performance

Metric	Base	Conservative	Aggressive
Integrated time-weighted absolute error (ITAE)	678	681	340
Exergy efficiency (%)	56.6	56.2	56.9
Max wall temperature (°C)	771	693	732
Setpoint Overshoot (%)	14.7	2.9	6.4

3.3 Creep-Fatigue Damage Accumulation Assessment

To assess the impact of the HTF mass flow rate control system on the creep and fatigue damage accumulation the model developed by Gentile et al. [4] was adopted considering the cloudy day flux maps described in Section 3.1. The analysis was performed assuming Alloy 800H as the tube material and calculating, for each panel of the eastern receiver flowpath, the number of days after which the interaction between creep and fatigue would lead to failure. Results, reported in Figure 5, show that with the base (PI) and conservative control systems the fifth panel of the flow path would fail at first, after 3285 and 3650 days respectively; when the aggressive control systems are considered the critical panel is the fourth and fifth and failure would occur after 5475 days.

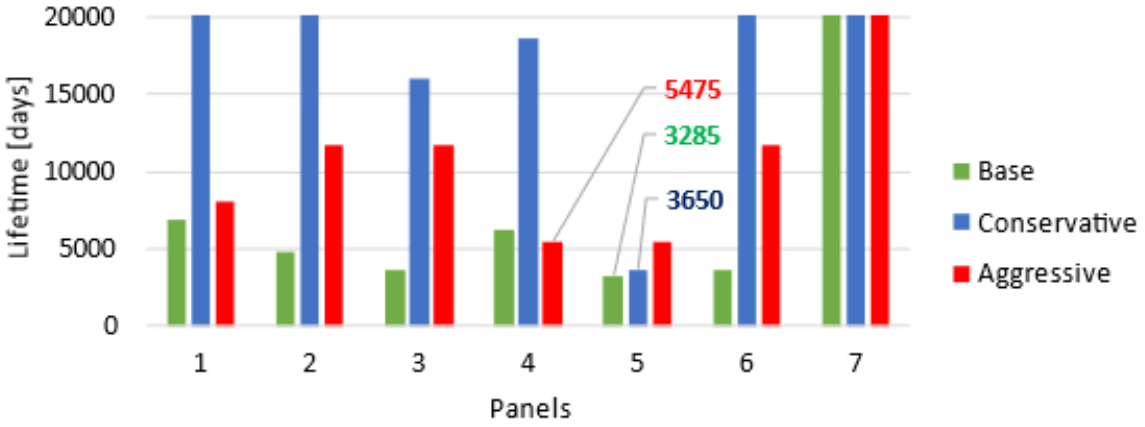

Figure 5. *Number of simulated days after which creep-fatigue failure would occur in each receiver panel (y-axis is limited to 20,000 days)*

To better understand whether the failure is caused by creep or fatigue, the creep-fatigue interaction diagrams reported in Figure 6a, b and c can be adopted. They show that failure is mainly driven by creep and fatigue when the base controller is adopted. When the conservative controller is considered, the lower wall temperature peaks leads to significantly better fatigue resistance and thus negligible fatigue damage. According to the creep-fatigue

damage assessment method [4], the fatigue properties of the material are conservatively evaluated at the maximum temperature experienced in each fatigue cycle, therefore the presence of temperature spikes significantly impact the mechanical properties. This results in creep being the major cause of failure. Lastly, when the aggressive controller is used, the maximum walls temperature are sufficiently high to limit the material fatigue resistance, thus fatigue is again an important driving factor in the creep-fatigue failure mode.

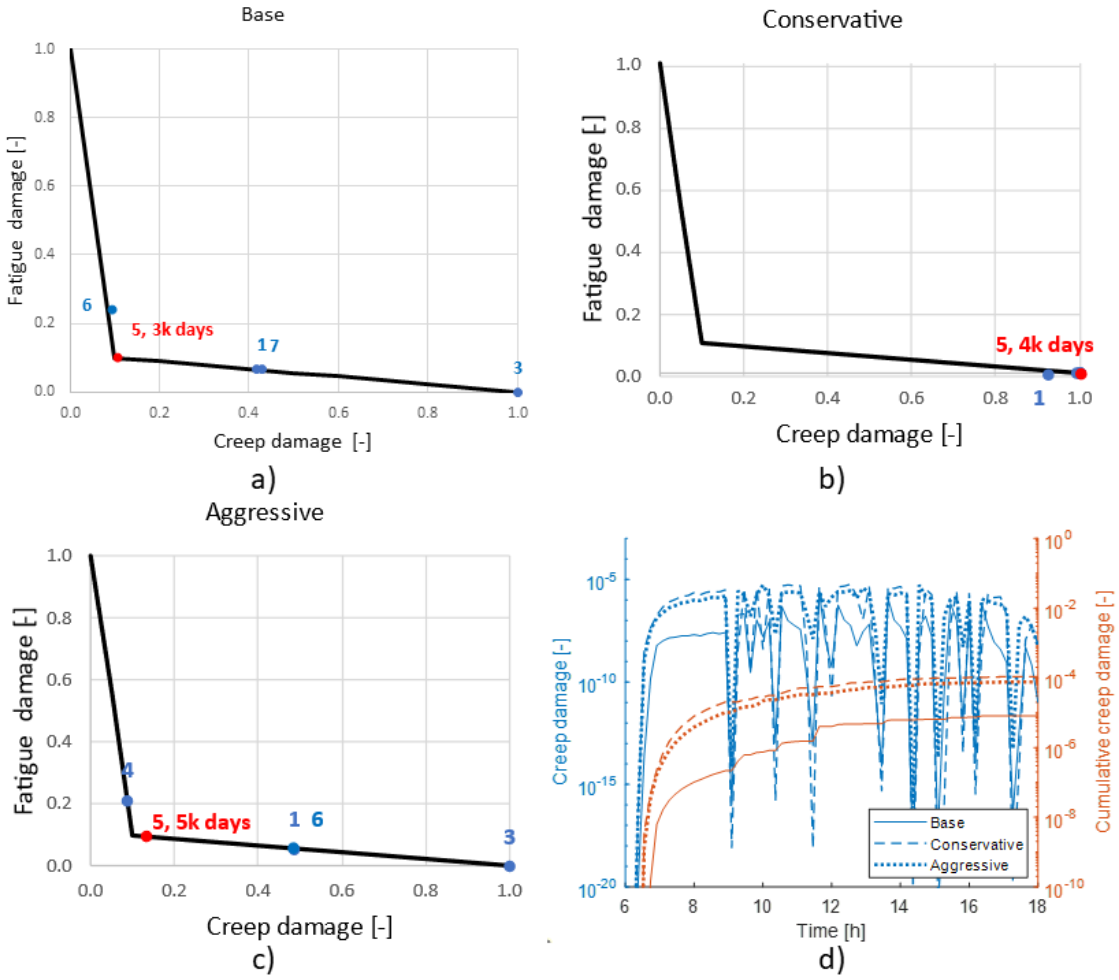

Figure 6. *Creep-fatigue interaction diagram*

Fig. 6d shows the instantaneous and cumulative creep damage accumulation during the investigated cloudy day in the last panel of the flow path (half of the tube, irradiated part). It is possible to notice how the conservative controller, which achieves the lowest wall temperatures, also leads to the highest creep damage due to its limited stress relaxation. On the contrary, the base controller which is characterized by the highest wall temperature, experiences the highest stress relaxation and thus the lowest creep damage accumulation.

4. Conclusion

A comparative analysis is performed against a conventional Proportional-Integral (PI) controller, focusing on energy performance and receiver lifespan. Leveraging a thermal Modelica model of the receiver, simulations are conducted for a solar tower plant resembling the 100 MW_{el} Crescent Dunes facility during a day with cloud cover. Both controllers employ feedforward MFR estimations derived from averaged DNI measurements, accounting for non-ideal inputs.

The conservative controller operates exclusively during clear sky conditions, employing a clear sky MFR during cloud transients to prevent receiver overheating post-cloud passage. In contrast, the aggressive controller integrates an adaptive predictive feedback system for temperature correction within the PI system, using outlet temperatures of receiver panels in conjunction with MFR to provide rapid response to cloud disturbances within the system.

Simulation results demonstrate precise setpoint tracking for both novel controllers, while the PI feedback-only controller struggles to achieve setpoint accuracy. The conservative controller exhibits satisfactory setpoint tracking during clear sky conditions with minimal overshoots during cloud transients. Meanwhile, the aggressive controller excels in setpoint tracking and demonstrates superior disturbance rejection during cloud transients, albeit with a minor increase in transient overshoots.

Lastly, the creep-fatigue damage accumulation in the receiver tubes was investigated for the three controllers, calculating for each of them the number of cloudy days after which the receiver would fail. Results showed that, with respect to the base controller the aggressive and conservative controllers showed a 67 % and 11 % relative increase in critical panel receiver lifetime when considering one cloudy day of simulation.

The methodology employed showcases the importance of controller operation on not only set point tracking and disturbance rejection performance but also the receiver failure mode and lifetime assessments.

Data availability statement

The data that support the findings of this study are available from the corresponding author, Gentile G., upon reasonable request.

Author contributions

C.B. Anderson: Conceptualization, Investigation, Methodology, Writing – Original Draft, Visualization, Formal analysis. **G. Gentile**: Conceptualization, Methodology, Software, Visualization, Formal analysis, Writing – Original Draft. **A. Longhi**: Conceptualization, Methodology, Software, Writing – Original Draft, Writing – Original Draft. **F. Casella**: Project administration, Conceptualization, Supervision. **M.E. Cholette**: Methodology, Supervision, Writing – Review & Editing. **G. Manzolini**: Project administration, Supervision, Writing – Review & Editing

Competing interests

The authors declare that they have no competing interests.

Acknowledgement

C.B. Anderson, and M.E. Cholette acknowledge the support of the Australian Government for this study, through the Australian Renewable Energy Agency (ARENA) and within the framework of the Australian Solar Thermal Research Initiative (ASTRI Project ID P54).

References

[1] R. W. Bradshaw et al., “Final Test and Evaluation Results from the Solar Two Project,” Contract, no. January, p. 294, 2002, doi: 10.2172/793226.

[2] B. Nouri et al., “Optimization of parabolic trough power plant operations in variable irradiance conditions using all sky imagers,” Solar Energy, vol. 198, no. December 2019, pp. 434–453, 2020, doi: 10.1016/j.solener.2020.01.045.

[3] S. Kannaiyan and N. D. Bokde, “Performance of Parabolic Trough Collector with Different Heat Transfer Fluids and Control Operation,” Energies (Basel), vol. 15, no. 20, Oct. 2022, doi: 10.3390/en15207572.

[4] G. Gentile, G. Picotti, M. Binotti, M. E. Cholette, and G. Manzolini, “Dynamic thermal analysis and creep-fatigue lifetime assessment of solar tower external receivers,” Solar Energy, . 247, no. May, pp. 408–431, 2022, doi: 10.1016/j.solener.2022.10.010.

[5] G. Gentile, G. Picotti, F. Casella, M. Binotti, M. E. Cholette, and G. Manzolini, “SolarReceiver2D: a Modelica Package for Dynamic Thermal Modelling of Central Receiver Systems,” IFAC-PapersOnLine, vol. 55, no. 20, pp. 259–264, 2022, doi: 10.1016/j.ifacol.2022.09.105.

[6] M. J. Wagner and T. Wendelin, “SolarPILOT: A power tower solar field layout and characterization tool,” Solar Energy, vol. 171, no. June, pp. 185–196, 2018, doi: 10.1016/j.solener.2018.06.063.

[7] W. T. Hamilton, M. J. Wagner, and A. J. Zolan, “Demonstrating SOLARPILOT’s Python Application Programmable Interface Through Heliostat Optimal Aimpoint Strategy Use Case,” Journal of Solar Energy Engineering, Transactions of the ASME, vol. 144, no. 3, pp. 1–7, 2022, doi: 10.1115/1.4053973.

[8] C. Maffezzoni, G. A. Magnani, and S. Quatela, “Process and Control Design of High-Temperature Solar Receivers: An Integrated Approach,” IEEE Trans Automat Contr, vol. AC-30, no. 3, pp. 194–209, 1985.